

# Mono- and Bilayered Lead(II)–bpno Polymers with Unusual Low Energy Emission Properties (bpno = 4,4'-Bipyridine *N,N'*-Dioxide)

Yanqing Xu,<sup>[a]</sup> Daqiang Yuan,<sup>[a]</sup> Lei Han,<sup>[a]</sup> En Ma,<sup>[a]</sup> Mingyan Wu,<sup>[a]</sup> Zhengzhong Lin,<sup>[a]</sup> and Maochun Hong<sup>\*[a]</sup>

**Keywords:** Lead complexes / 4,4'-Bipyridine *N,N'*-dioxide / Coordination polymers / Phosphorescence

Reaction of 4,4'-bipyridine *N,N'*-dioxide (bpno) and lead(II) nitrate with or without dicyanamido ions (dca) in aqueous solution yielded polymeric complexes {Pb<sub>2</sub>(bpno)<sub>4</sub>(dca)<sub>2</sub>·(NO<sub>3</sub>)<sub>2</sub>Pb<sub>2</sub>(bpno)<sub>4</sub>(NO<sub>3</sub>)<sub>4</sub>·5H<sub>2</sub>O}<sub>n</sub> (**1**) and {Pb(bpno)(NO<sub>3</sub>)<sub>2</sub>·H<sub>2</sub>O}<sub>n</sub> (**2**), respectively. The single-crystal X-ray analyses show that the structures of both complexes consist of dinuclear Pb<sup>II</sup> units which are bridged through bpno ligands in novel modes to extend their topologies. Compound **1** exhibits a bilayered rhombus grid, while **2** displays a monolayered

rhombus grid. The different excitations of solid samples of **1** and **2**, at room temperature, produced intense emission bands which are almost the same in appearance with peak maxima at 616 nm and 617 nm, respectively. Both low-energy emissions were determined to be phosphorescence by their long decay lifetime at room temperature.

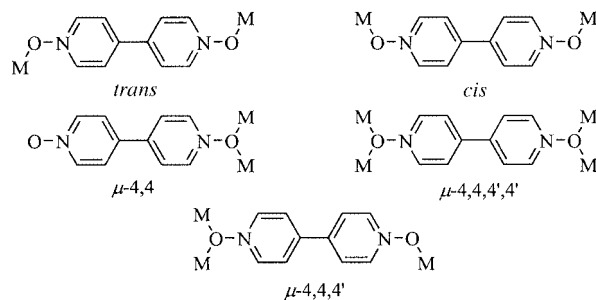
(© Wiley-VCH Verlag GmbH & Co. KGaA, 69451 Weinheim, Germany, 2005)

## Introduction

The s<sup>2</sup> materials can be important in applications like electroluminescent devices<sup>[1]</sup> or organic light-emitting diode (OLED) technology etc.,<sup>[2]</sup> and so have stimulated many scientists' interest. As far as the intrinsic appeal of Pb<sup>2+</sup> is concerned, the presence of an 6s<sup>2</sup> outer electron configuration not only leads to interesting topological arrangements,<sup>[3]</sup> but also plays an important role in the luminescence action of the complex.<sup>[4]</sup> Consequently, a remarkable amount of studies have been done on the optical properties of lead(II) centers.<sup>[5]</sup> In 1986 R. Ballardini et al. reported that the Pb(8-quinolinolate)<sub>2</sub> chelates exhibit a very weak red intraligand (IL) phosphorescence in addition to a much stronger green IL fluorescence in fluid solution.<sup>[6]</sup> S. K. Dutta et al. further put forward that Pb<sup>2+</sup> could act as its own luminescent sensor via the highly luminescent lead halide cluster Pb<sub>4</sub>Br<sub>11</sub><sup>3-</sup> due to a delocalized cluster state.<sup>[5b]</sup> More recent studies by A. Strasser and A. Vogler focused on IL phosphorescence research of the lead(II) β-diketonates at both low temperatures and room temperature.<sup>[7]</sup> In fact, little attention has been focused on luminescent lead polymers even though there are many interesting structure reports. Taking into account that the presence of lead in coordination polymers will reduce the radiative lifetime of

triplets by increased spin-orbit coupling and generate a room-temperature phosphorescence, as is largely related to the application of triplet emitters in OLED technology, we have recently become interested in the phosphorescence properties of lead coordination polymers.

On the other hand, 4,4'-bipyridine *N,N'*-dioxide (bpno) possesses a longer bridging spacer and richer coordination modes, compared with 4,4'-bipyridine. As shown in Scheme 1, there are five possible kinds of connection modes for the bpno ligand.<sup>[8]</sup> The *cis* and *trans* modes have been observed in many compounds.<sup>[9]</sup> The four-connecting coordination mode (μ-4,4,4',4') was newly found in La–bpno.<sup>[10]</sup> However, the three-connecting mode (μ-4,4,4') remains unknown. Another ligand, the dicyanamido ion (dca), also exhibits various coordination modes, which makes it a fairly good building block for crystal engineering.<sup>[11]</sup> By the self-assembly of bpno and/or dca ligands with transition metal ions, coordination frameworks with larger cavities or channels may be expected.<sup>[12]</sup> Thus, by the reaction of Pb<sup>2+</sup> and



Scheme 1. Schematic illustration showing the coordination modes of bpno.

[a] State Key Laboratory of Structural Chemistry, Fujian Institute of Research on the Structure of Matter, Chinese Academy of Sciences, Fuzhou, Fujian 350002, China  
Fax: +86-591-83714946  
E-mail: hmc@ms.fjirsm.ac.cn

Supporting information for this article is available on the WWW under <http://www.eurjic.org> or from the author.

bpno with or without dca, two novel polymeric complexes,  $\{\text{Pb}_2(\text{bpno})_4(\text{dca})_2(\text{NO}_3)_2\text{Pb}_2(\text{bpno})_4(\text{NO}_3)_4 \cdot 5\text{H}_2\text{O}\}_n$  (**1**), and  $\{\text{Pb}(\text{bpno})(\text{NO}_3)_2 \cdot \text{H}_2\text{O}\}_n$  (**2**) were obtained. Herein, we wish to report their syntheses, crystal structures, TG, IR spectroscopic and luminescent properties. To the best of our knowledge, the three-connecting mode ( $\mu$ -4,4,4') has been confirmed for the first time in both compounds.

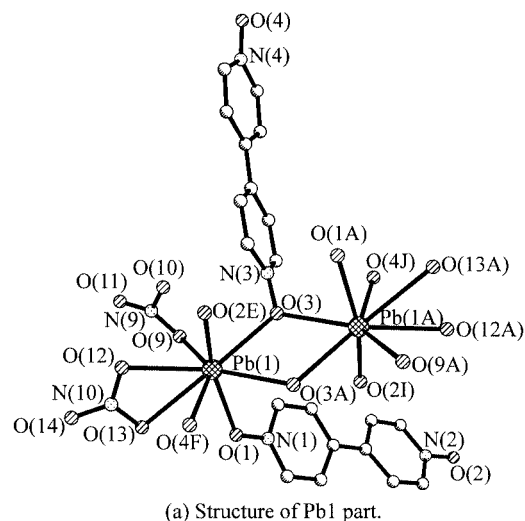
## Results and Discussion

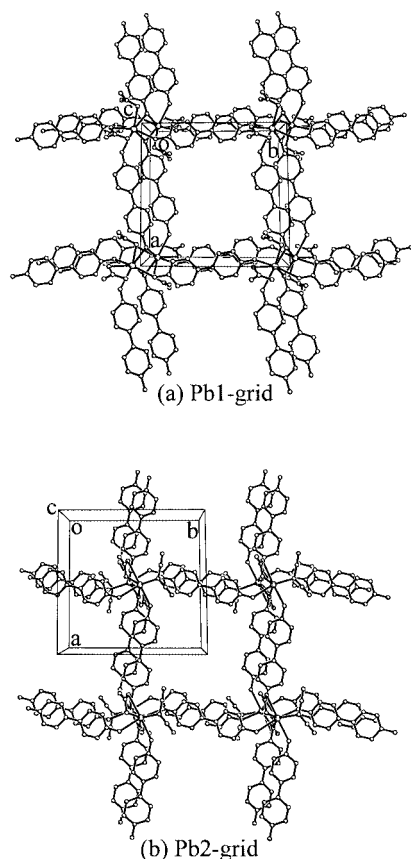
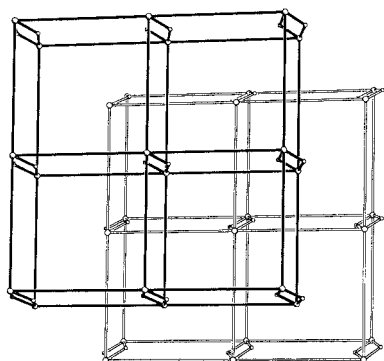
Heating of the mixture of 4,4'-bpno, dca and  $\text{Pb}(\text{NO}_3)_2 \cdot 2\text{H}_2\text{O}$  in a methanol solution led to yellow prismatic crystals of compound **1**, while heating of the mixture of 4,4'-bpno and  $\text{Pb}(\text{NO}_3)_2 \cdot 2\text{H}_2\text{O}$  in a methanol solution led to orange prismatic crystals of compound **2**. Single crystal analyses show that both complexes have polymeric structures based on dinuclear  $\text{Pb}^{\text{II}}$  units bridged by bpno ligands.

### Crystal Structure of Compound 1

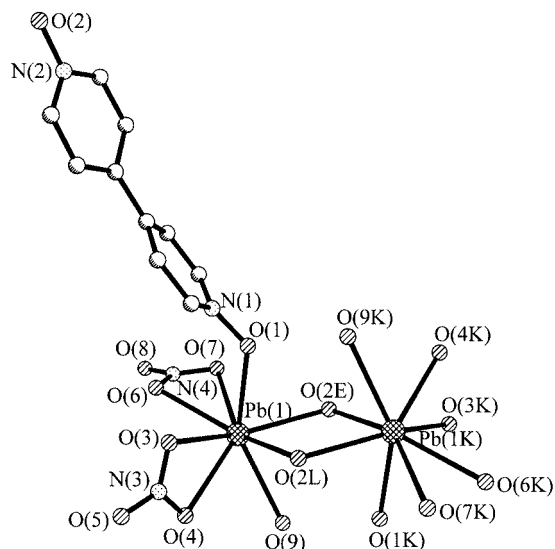
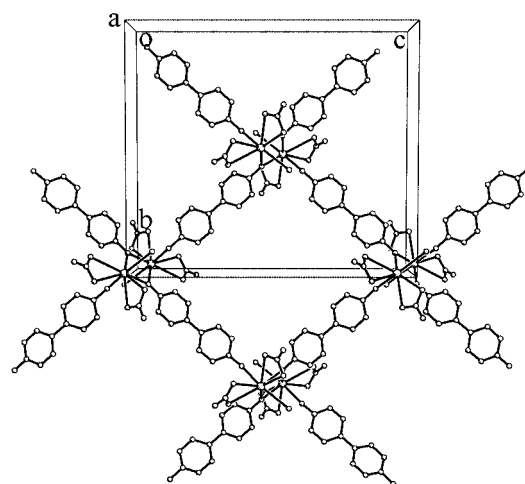
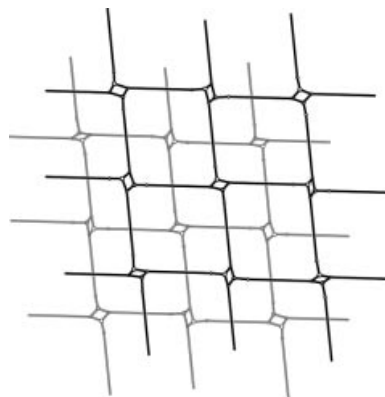
The asymmetric unit of compound **1** consists of two crystallographically independent lead(II) motifs, as well as two and a half free lattice water molecules. As shown in Figure 1a, Pb1 is in an eight-coordinate environment, surrounded only by O atoms, of which five are from bpno ligands, two from a bidentate  $\text{NO}_3^-$  and one from a monodentate  $\text{NO}_3^-$  group. Pb1 atoms are linked by the O(3) atoms of the bpno groups, forming a planar four-membered ring  $\text{Pb}(1)\text{--O}(3)\text{--Pb}(1\text{A})\text{--O}(3\text{A})$  with  $\text{O--Pb--O}$  bond angles of  $62.93^\circ$  and  $\text{Pb--O--Pb}$  bond angles of  $117.07^\circ$ . This  $\text{Pb}_2\text{O}_2$  unit is nearly symmetric with the  $\text{Pb--O}$  distances being  $2.633(9)$  Å for  $\text{Pb}(1)\text{--O}(3)$  and  $2.690(10)$  Å for  $\text{Pb}(1)\text{--O}(3\text{A})$ , respectively. The  $\text{Pb--}(\mu\text{-O})$  bond lengths are comparable to those found in other crystallographically characterized  $\text{Pb}_2(\mu\text{-OR})_2$  systems.<sup>[3d,13]</sup> The distance between the two nonbonded Pb atoms [ $\text{Pb}(1)\text{--Pb}(1\text{A})$ ] is about  $4.541$  Å. The  $\text{Pb}_2\text{O}_2$  units are bridged by two parallel bpno ligands along the *oa* direction with  $\text{Pb}(1)\text{--O}(4\text{F})$  [ $2.511(11)$  Å] and  $\text{N}(3)\text{--O}(3)$  [ $1.317(14)$  Å] yielding a double-stranded chain, in which bpno adopts both  $\mu$ -4,4,4' and *trans* connection modes. It is noted that bonding in the  $\mu$ -4,4,4' mode is exclusive and has been observed in the structure of **1** for the first time. These adjacent chains are further linked through double bpno ligands along the *ob* direction with  $\text{Pb}(1)\text{--O}(2\text{D})$  [ $2.461(10)$  Å] and  $\text{Pb}(1)\text{--O}(1)$  [ $2.647(10)$  Å] leading to a 2D bilayered coordination network as illustrated in Figure 2a.

The dca ligand is not involved in the Pb1 motif but is in the Pb2 part (Figure 1b). The Pb2 part also adopts an eight-coordinate geometry. Because of the existence of the dca ligand, there is only one  $\text{NO}_3^-$  ion involved in the coordination sphere, which adopts a chelating coordination mode and occupies two coordination points. The dca ligand in this structure bonds to the Pb atom by its amine nitrogen but not the nitrile nitrogen atom. The extended structure is shown in Figure 2b, and no significant differences are observed between the Pb2 and Pb1 grids except that one  $\text{NO}_3^-$



Figure 2. View of the 2D sheet of compound **1**.Figure 3. Schematic view of the packed structure in compound **1** ignoring free water molecules.

molecule. Although the  $\text{Pb}_2(\mu\text{-4,4,4'-'bpno})_2$  unit is again found in this structure, except for the absence of two bpno ligands (contrasted with **1**), the extended structure only leads to a monolayer topology with the dimensions of a rhombus grid  $13.814 \times 13.814 \text{ \AA}$  (Figure 5). All bpno ligands in **2** adopt a  $\mu\text{-4,4,4'-'}$  connection mode. As a result of compact stacking in crystallography, the dimension of the open framework is also to be reduced (Figure 6).

Figure 4. Diagram showing the structure of compound **2**, hydrogen atoms are omitted. Symmetry code: E:  $-x, y + 1/2, -z + 1/2$ ; L:  $x, -y + 1/2, z + 1/2$ ; K:  $-x, -y+1, -z+1$ .Figure 5. View of the 2D sheet of compound **2**.Figure 6. Schematic view of the packed structure in compound **2**.

## IR Spectroscopy

The infrared spectra of solid samples of **1** and **2** are notably different apart from the characteristic bands of the organic ligand. Compound **1** displays absorption peaks at 2257, 2194 and 2144  $\text{cm}^{-1}$ , which correspond to  $\nu_{\text{sym}} + \nu_{\text{asym}}(\text{C}\equiv\text{N})$ ,  $\nu_{\text{sym}}(\text{C}\equiv\text{N})$  and  $\nu_{\text{asym}}(\text{C}\equiv\text{N})$  of the dca ligand. The values of the stretching frequencies are relatively lower than those of Na(dca), observed at 2286, 2232 and 2179  $\text{cm}^{-1}$ .<sup>[14]</sup> The shift towards lower frequencies of these peaks reflects the coordination mode of dca through the amide nitrogen atom, which results in decreasing electron density at the cyano groups.<sup>[15]</sup> A broad absorption band at 3400  $\text{cm}^{-1}$  assigned to  $\nu(\text{OH})$  appears in the spectra, showing the presence of water molecules in both complexes.

## Luminescence Properties

Figure 7 shows the emission spectra of **1** and **2** measured at room temperature. The emission spectra of both compounds are dominated by an intense and broad emission band at  $\lambda = 616 \text{ nm}$  for **1** ( $\lambda_{\text{ex}} = 388 \text{ nm}$ ) and  $\lambda = 617 \text{ nm}$  for **2** ( $\lambda_{\text{ex}} = 510 \text{ nm}$ ). The further lifetime measurements at room temperature of each emission maximum gave the results 17.89  $\mu\text{s}$  for **1** and 3.50  $\mu\text{s}$  for **2**. Based on their  $10^{-5}$ – $10^{-6}$  s range lifetime at room temperature, both low-energy emissions could be determined to be phosphorescence, as is consistent with the general idea that the appearance of a room-temperature phosphorescence requires the presence of a heavy metal ion which reduces the radiative lifetime of triplets by increased spin-orbit coupling.<sup>[7b]</sup> Commonly, the emitting triplets are frequently of the CT (charge transfer) or IL (intraligand) type while LF (ligand field) states are mostly deactivated by radiationless processes.<sup>[7b]</sup> In order to assign the type of the luminescence, luminescent measurements were taken of both free bpno ligand and bpno complexes. The free bpno ligand in the solid state at room temperature was found to emit at 459 nm under 396 nm radiation (see Figure S1; Supporting Information). But bpno in the *cis* mode (see Scheme 1) was reported to be incapable of activating emission from  $\text{Eu}^{\text{III}}$  in a one-dimensional coordination polymer.<sup>[16]</sup> We have also reported a mononuclear complex  $[\text{Cd}(\text{dca})_2(\text{bpno})_2 \cdot (\text{H}_2\text{O})_2]$ ,<sup>[17]</sup> in which bpno acts as a terminal ligand. The recent emission measurement on it showed a narrow emissive band at 399 nm ( $\lambda_{\text{ex}} = 376 \text{ nm}$ ) (see Figure S2; Supporting Information). From the above measurements, we feel confident to surmise that as an organic fluorophore, the emission action of bpno may vary with the change of the coordination mode and the coordinated metal ion. As a result, increased spin-orbit coupling induced by the heavy-atom effect of lead(II) facilitates intersystem crossing, and the IL phosphorescence is fast enough to successfully compete with radiationless deactivations.<sup>[7a]</sup> In addition, the  $(\mu\text{-}4,4,4'\text{-bpno})_2\text{Pb}_2$  dinuclear cluster cannot be neglected in both structures. From the lead halide cluster  $\text{Pb}_4\text{Br}_{11}^{3-}$  it has been reported that the charge transfer states and states delocalized over the bromide-bridged lead ions are important.<sup>[5b]</sup> Comparably, the emis-

sions in this work may be assigned partly to the delocalized cluster state of the oxygen-bridged lead ions. To the best of our knowledge, such a long lifetime and low-energy luminescence has never been reported for  $\text{Pb}^{2+}$  coordination polymers. This study suggests that bpno is an appropriate ligand for lead complexes to generate room-temperature phosphorescence, and the results are interesting for finding the long-lived room-temperature phosphorescence relating to  $\text{Pb}^{2+}$  coordination polymers. We are actively moving towards other related bpno and heavy main group metals with  $s^2$  electron configurations in order to make further progress on the molecule-based functional solids.

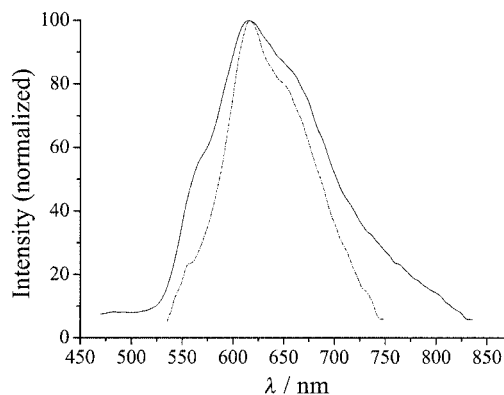


Figure 7. Emission measured for **1** ( $\lambda_{\text{ex}} = 388 \text{ nm}$ ) and **2** ( $\lambda_{\text{ex}} = 510 \text{ nm}$ ) at room temperature. Solid line for compound **1** and dash-dotted line for **2** and normalized at maximum intensity.

## TGA Study

To access the thermal stability of the two compounds, TG analyses were carried out. The TGA diagrams of the crystalline samples showed weight loss in the temperature range 90–165 °C in **1**, corresponding to five free water molecules (3.19%; calculated 3.07%). The anhydrous compound began to decompose at 260 °C. However, the decomposition was still not complete at 800 °C, as could be confirmed by the black color of the residual and the slope of the TGA curves.

For compound **2**, only one coordination aqua ligand exists in the structure. The weight loss was found to be 3.42% in the range of 80–110 °C, which is a little higher than the calculated value of 3.35%. The weight was unchanged until the temperature increased to 309 °C, indicating that the thermal stability of **2** is higher than **1**. Similarly for compound **1**, the decomposition process was incomplete, which was also confirmed by the black color of the residual and the slope of the TGA curves.

## Conclusions

In summary, two novel luminescent  $\text{Pb}^{\text{II}}$  coordination polymers with different types of layered grid structures were synthesized. This paper investigated the microscopic features of molecular packing, the luminescent essence and the thermal stability of both compounds. These results are



interesting not only for confirming new coordination modes of bpno for the first time, but also for finding the long-lived phosphorescence at room temperature emitted from lead coordination polymers, which may have some potential application in OLED technology. Further studies on analogous functional solids will be carried out in the proceeding work.

## Experimental Section

**General:** All chemicals were of reagent-grade quality obtained from commercial sources and used without further purification. Elemental analyses were performed with a German Elementary Varil EL III instrument. IR spectra were recorded in the range 4000–400  $\text{cm}^{-1}$  with a Magna 750 FT-IR spectrometer using KBr pellets. TGA analyses were carried out with a Netzsch STA449C unit, at a heating rate of 15  $^{\circ}\text{Cmin}^{-1}$  under nitrogen from 30 to 800  $^{\circ}\text{C}$ . Fluorescent spectra were measured at room temperature with an Edinburgh FL-FS90 TCSPC system.

**Synthesis of 1 and 2:** Ligand 4,4'-bpno (0.25 mmol, 0.056 g) and  $\text{Pb}(\text{NO}_3)_2 \cdot 2\text{H}_2\text{O}$  (0.25 mmol, 0.042 g) were mixed in a methanol (20 mL) solution. Ligand dca (0.50 mmol, 0.045 g) was added to the above solution. The mixture was heated for 15 min with stirring and then filtered. Slow concentration of the filtrate at room temperature led to yellow prismatic crystals of compound **1**. Yield: 0.105 g, 58%. Compound **2** was synthesized by the same procedure as above but without the addition of dca. The resulting solution was allowed to stand at room temperature. Orange prismatic crystals were obtained after 2 d. Yield: 0.088 g, 65%. **1**:  $\text{C}_{84}\text{H}_{74}\text{N}_{28}\text{O}_{39}\text{Pb}_4$  (2928.47): calcd. C 34.40, H 2.55, N 13.38; found C 34.38, H 2.58, N 13.37. IR (KBr):  $\tilde{\nu}$  = 3434 (m), 3098 (m), 3064 (m), 3036 (w), 2257 (m), 2194 (m), 2144 (s), 1625 (m), 1545 (m), 1477 (vs), 1384 (vs), 1351 (s), 1240 (s), 1221 (vs), 1184 (vs), 1026 (s), 834 (s), 699 (m), 548 (s), 517 (w), 478 (m)  $\text{cm}^{-1}$ . **2**:  $\text{C}_{10}\text{H}_{10}\text{N}_4\text{O}_9\text{Pb}$  (537.41): calcd. C 22.30, H 1.87, N 10.41; found C 22.31, H 1.89, N 10.39. IR (KBr):  $\tilde{\nu}$  = 3445 (m), 3099 (m), 3074 (m), 3038 (w), 1624 (w), 1545 (m), 1478 (vs), 1380 (vs), 1348 (s), 1243 (s), 1224 (vs), 1183 (vs), 1027 (s), 836 (s), 700 (m), 548 (s), 515 (m), 477 (m)  $\text{cm}^{-1}$ .

**Crystal Structure Characterization:** Single crystals of the compounds with approximate dimensions 0.22 mm  $\times$  0.19 mm  $\times$  0.17 mm for **1** and 0.19 mm  $\times$  0.16 mm  $\times$  0.15 mm for **2** were coated with epoxy glue and mounted on a glass fiber in a random orientation for data collections. The intensity data were collected with a Smart CCD diffractometer with graphite-monochromated  $\text{Mo-K}\alpha$  ( $\lambda$  = 0.71073 Å) radiation at room temperature in the  $\omega$ -2 $\theta$  scan mode. An empirical absorption correction was applied to the data using the SADABS program.<sup>[18]</sup> The structures were solved by direct methods and refined on  $F^2$  by full-matrix least-squares, employing the SHELXTL program.<sup>[19]</sup> All non-hydrogen atoms were refined with anisotropic thermal parameters. H atoms bonded to C atoms were positioned geometrically (C–H bond fixed at 0.93 Å) and H atoms bonded to O atoms were placed at calculated positions by the HYDROGEN computer program (O–H bond fixed at 0.85 Å),<sup>[20]</sup> assigned isotropic displacement parameters and allowed to ride on their respective parent atoms. Crystal data and structure refinement parameters are summarized in Table 1. Selected bond lengths and angles are presented in Table 2. CCDC-236662 (**1**) and -236663 (**2**) contain the supplementary crystallographic data for this paper. These data can be obtained free of charge from The Cambridge Crystallographic Data Centre via [www.ccdc.cam.ac.uk/data\\_request/cif](http://www.ccdc.cam.ac.uk/data_request/cif).

Table 1. Crystal data and structure refinement for compounds **1** and **2**.

	<b>1</b>	<b>2</b>
Empirical formula	$\text{C}_{84}\text{H}_{74}\text{N}_{28}\text{O}_{39}\text{Pb}_4$	$\text{C}_{10}\text{H}_{10}\text{N}_4\text{O}_9\text{Pb}$
Formula mass	2928.47	537.41
Space group	$P\bar{1}$	$Pbca$
$a$ [Å]	13.4650(3)	7.8957(5)
$b$ [Å]	13.4669(2)	18.1502(1)
$c$ [Å]	13.7977(3)	20.8299(8)
$\alpha$ [°]	85.4380(10)	90
$\beta$ [°]	76.2910(10)	90
$\gamma$ [°]	88.4590(10)	90
$V$ [Å <sup>3</sup> ]	2422.9(1)	2985.1(3)
$Z$	1	8
$\rho$ (calcd.) [g $\text{cm}^{-3}$ ]	2.007	2.392
$\mu$ [mm <sup>-1</sup> ]	7.034	11.361
Goodness-of-fit on $F^2$	1.100	1.162
Final $R$ indices [ $I > 2\sigma(I)$ ] <sup>[a]</sup>	$R_1 = 0.0687$ , $wR_2 = 0.1181$	$R_1 = 0.0491$ , $wR_2 = 0.1157$
$R$ indices (all data)	$R_1 = 0.1127$ , $wR_2 = 0.1389$	$R_1 = 0.0718$ , $wR_2 = 0.1300$

[a]  $R_1 = \Sigma(|F_o| - |F_c|)/\Sigma|F_o|$ , and  $wR_2 = \{\Sigma[w(F_o^2 - F_c^2)^2]/\Sigma[w(F_o^2)^2]\}^{1/2}$  with  $w = 1/\sigma^2(F_o^2) + (aP)^2 + bP$ , where  $P = (F_o^2 + 2F_c^2)/3$ .

Table 2. Selected bond lengths [Å] and angles [°] for compounds **1** and **2**.

<b>1</b> <sup>[a]</sup>			
Pb(1)–O(2D)	2.461(10)	O(3)–Pb(1)–O(3A)	62.9(4)
Pb(1)–O(4F)	2.511(11)	O(12)–Pb(1)–O(13)	45.8(3)
Pb(1)–O(3)	2.633(9)	O(2D)–Pb(1)–O(4F)	80.3(3)
Pb(1)–O(1)	2.647(10)	O(3)–Pb(1)–O(1)	98.8(3)
Pb(1)–O(12)	2.674(11)	O(4F)–Pb(1)–O(3)	137.4(4)
Pb(1)–O(3A)	2.690(10)	O(4F)–Pb(1)–O(1)	92.3(3)
Pb(1)–O(9)	2.754(19)	O(1)–Pb(1)–O(3A)	84.3(3)
Pb(1)–O(13)	2.827(14)	O(4F)–Pb(1)–O(3A)	77.7(4)
Pb(2)–O(5)	2.473(10)	O(7B)–Pb(2)–O(7)	65.4(3)
Pb(2)–O(8C)	2.486(10)	O(16)–Pb(2)–O(15)	43.7(4)
Pb(2)–O(6D)	2.560(10)	O(6D)–Pb(2)–O(7)	80.2(3)
Pb(2)–O(7B)	2.622(10)	O(5)–Pb(2)–O(6D)	157.7(4)
Pb(2)–O(7)	2.643(9)	O(5)–Pb(2)–O(8C)	82.6(3)
Pb(2)–O(16)	2.818(12)	O(7)–Pb(2)–N(13)	132.3(3)
Pb(2)–N(13)	2.824(14)	O(7B)–Pb(2)–N(13)	141.6(4)
Pb(2)–O(15)	2.829(15)	O(8C)–Pb(2)–O(6D)	90.8(3)
<b>2</b> <sup>[a]</sup>			
Pb(1)–O(1)	2.538(8)	O(2L)–Pb(1)–O(2E)	69.8(3)
Pb(1)–O(2L)	2.541(8)	O(4)–Pb(1)–O(3)	47.8(3)
Pb(1)–O(2E)	2.575(8)	O(6)–Pb(1)–O(7)	46.3(3)
Pb(1)–O(6)	2.638(8)	O(1)–Pb(1)–O(2E)	77.0(3)
Pb(1)–O(4)	2.643(9)	O(1)–Pb(1)–O(2L)	78.3(3)
Pb(1)–O(3)	2.676(11)	O(1)–Pb(1)–O(9)	147.4(3)
Pb(1)–O(9)	2.740(9)	O(2L)–Pb(1)–O(9)	77.0(3)
Pb(1)–O(7)	2.828(10)	O(2E)–Pb(1)–O(9)	74.9(3)

[a] Symmetry transformations used to generate equivalent atoms: A:  $-x + 2, -y, -z + 1$ ; B:  $-x + 1, -y + 1, -z$ ; C:  $x + 1, y, z$ ; D:  $x, y + 1, z$ ; E:  $-x, y + 1/2, -z + 1/2$ ; F:  $x - 1, y, z$ ; L:  $x, -y + 1/2, z + 1/2$ .

## Acknowledgments

We are grateful to the National Natural Science Foundation of China (project 20231020) and the Natural Science Foundation of Fujian Province for financial support.

- [1] a) T. Tsuboi, P. Sifsten, *Phys. Rev. B* **1991**, *43*, 1777–1780; b) A. A. Bol, A. Meijerink, *Phys. Stat. Solidi B* **2001**, *1*, 173–177; c) A. A. Bol, A. Meijerink, *Phys. Chem. Chem. Phys.* **2001**, *3*, 2105–2112; d) P. Singh, M. M. Richter, *Inorg. Chim. Acta* **2004**, *357*, 1589–1592.
- [2] S. Miyata, H. S. Nalwa (Eds.), *Organic Electroluminescent Materials and Devices*, Gordon and Breach, New York, **1997**.
- [3] a) C. S. Weinert, I. A. Guzei, A. L. Rheingold, L. R. Sita, *Organometallics* **1998**, *17*, 498–500; b) M. H. Jack, M. Saeed, A. S. Ali, *Inorg. Chem.* **2004**, *43*, 1810–1812; c) Y. J. Shi, L. H. Li, Y. Z. Li, X. T. Chen, Z. L. Xue, X. Z. You, *Polyhedron* **2003**, *22*, 917–923; d) L. A. Hall, D. J. Williams, S. Menzer, A. J. P. White, *Inorg. Chem.* **1997**, *36*, 3096–3101.
- [4] a) S. Deo, H. A. Godwin, *J. Am. Chem. Soc.* **2000**, *122*, 174–175; b) J. Li, Y. Lu, *J. Am. Chem. Soc.* **2000**, *122*, 10466–10467; c) P. C. Ford, A. Vogler, *Acc. Chem. Res.* **1993**, *26*, 220–226; d) H. Y. Duan, X. P. Ai, Z. K. He, *Spectrochim. Acta A* **2003**, *60*, 1447–1451.
- [5] a) H. Nikol, A. Vogler, *J. Am. Chem. Soc.* **1991**, *113*, 8988–8990; b) S. K. Dutta, M. W. Perkovic, *Inorg. Chem.* **2002**, *41*, 6938–6940.
- [6] R. Ballardini, G. Varani, M. T. Indelli, F. Scandola, *Inorg. Chem.* **1986**, *25*, 3858–3865.
- [7] a) A. Strasser, A. Vogler, *J. Photochem. Photobiol. A* **2004**, *165*, 115–118; b) A. Strasser, A. Vogler, *Inorg. Chem. Commun.* **2004**, *7*, 528–530.
- [8] B. Q. Ma, H. L. Sun, S. Gao, G. X. Xu, *Inorg. Chem.* **2001**, *40*, 6247–6253.
- [9] a) D. L. Long, A. J. Blake, N. R. Champness, C. Wilson, M. Schroder, *Chem. Eur. J.* **2002**, *8*, 2026–2033; b) D. L. Long, A. J. Blake, N. R. Champness, C. Wilson, M. Schroder, *J. Am. Chem. Soc.* **2001**, *123*, 3401–3402; c) S. Tanase, M. Andruh, A. Müller, M. Schmidtman, C. Mathonière, G. Rombaut, *Chem. Commun.* **2001**, *12*, 1084–1085.
- [10] S. L. Ma, W. X. Zhu, G. H. Huang, D. Q. Yuan, X. Yan, *J. Mol. Struct.* **2003**, *646*, 89–94.
- [11] a) E. Colacio, F. Lloret, E. Ben Maimoun, R. Kivekäs, R. Silanpää, J. Suárez-Varela, *Inorg. Chem.* **2003**, *42*, 2720–2724; b) J. L. Manson, J. Y. Gu, J. A. Schlueter, H. H. Wang, *Inorg. Chem.* **2003**, *42*, 3950–3955; c) J. H. Luo, M. C. Hong, R. H. Wang, R. Cao, Q. Shi, J. B. Weng, *Eur. J. Inorg. Chem.* **2003**, *9*, 1778–1784.
- [12] a) B. Q. Ma, S. Gao, H. L. Sun, G. X. Xu, *J. Chem. Soc. Dalton Trans.* **2001**, 130–133; b) A. Nedelcu, Z. Žak, A. M. Madalan, J. Pinkas, M. Andruh, *Polyhedron* **2003**, *22*, 789–794.
- [13] a) P. Bhattacharyya, J. Parr, A. M. Z. Slawin, *Inorg. Chem. Commun.* **1999**, *2*, 113–115; b) S. S. Tandon, V. McKee, *J. Chem. Soc. Dalton Trans.* **1989**, *1*, 19–24.
- [14] M. Hvastijová, J. Kohout, M. Okruhlica, J. Mrozinski, L. Jäger, *Transition Met. Chem.* **1993**, *18*, 579–582.
- [15] S. R. Marshall, C. D. Incarvito, W. W. Shum, A. L. Rheingold, J. S. Miller, *Chem. Commun.* **2002**, *24*, 3006–3007.
- [16] C. Seward, S. Wang, *Can. J. Chem.* **2001**, *79*, 1187–1193.
- [17] Y. Q. Xu, D. Q. Yuan, Y. Xu, W. H. Bi, Y. F. Zhou, M. C. Hong, *Acta Crystallogr., Sect. E* **2004**, *60*, m713–m714.
- [18] G. M. Sheldrick, *SADABS, A Program for Empirical Absorption Correction*, University of Göttingen, Germany, **1998**.
- [19] G. M. Sheldrick, *SHELXTL, Crystallographic Software Package*, version 5.1, Bruker-AXS, Madison, WI, **1998**.
- [20] a) M. Nardelli, *J. Appl. Crystallogr.* **1999**, *32*, 563–571; b) L. J. Farrugia, *J. Appl. Crystallogr.* **1999**, *32*, 837–838.

Received: November 1, 2004